Electronic Supplementary Material (ESI) for RSC Advances

Supporting Information (RSC Advances)

Manipulate Light Emission of Quantum Dots by Simultaneously Controlling Crystal Morphology and Doping

Hsueh-Shih Chen, Bertrand Lo and Jhen-Yu Huang

Layer-by-layer doping.[1] ZnSe cores were first produced. Then, several sets of alternating impurity monomer (TOPSe-I) injection and host monomer (TOPSe) injection were conducted to overcoat ZnSe cores. Zn precursor was prepared by mixing 2.5 mmol ZnO, 8 mmol lauric acid and 8 mmol hexadecylamine at 280 °C under argon. The TOPSe was prepared by dissolving 1.5 mol Se into 1 ml TOP and diluted by toluene to 5 ml. The TOPSe-I was prepared by 0.1 mmol iodine (degassed in vacuum for 1 hour), 1.5 mmol Se, 1 ml TOP, 5 ml toluene in ultrasonic bath at 50 ^{o}C. ZnSe cores were produced by injecting 1 ml of the TOP-Se into the Zn precursor at 280 ^{o}C, followed by growing at 260 ^{o}C for about 2 min. Alternating TOPSe-I (0.5 ml) and TOPSe (0.5 ml) injections were carried out every 30 s. Each injection of TOPSe-I contained 0.01 mmol iodine atoms (monomer concentration I/Zn = 0.4 mol%). After reaction and the system cooled to room temperature, 50 ml methanol was added into the vessel under argon flow at 150 ^{o}C, followed by an ultrasonic bath for 60 min. Solids precipitated by centrifugation were further washed in warm methanol at 50 ^{o}C for three times and finally dried in vacuum for 1 h.

Conventional mix-doping. ZnSe:I QDs prepared by a monomers mixing method with a mixture of TOP-Se (Se/TOP = 1.5 mol/1 ml) and TOP-I (iodine/TOP/toluene = 0.1 mmol/1 ml TOP/1 ml toluene) are named mix-ZnSe:I QDs. Injection and growth temperatures were 280 ^{o}C and 260 ^{o}C respectively.

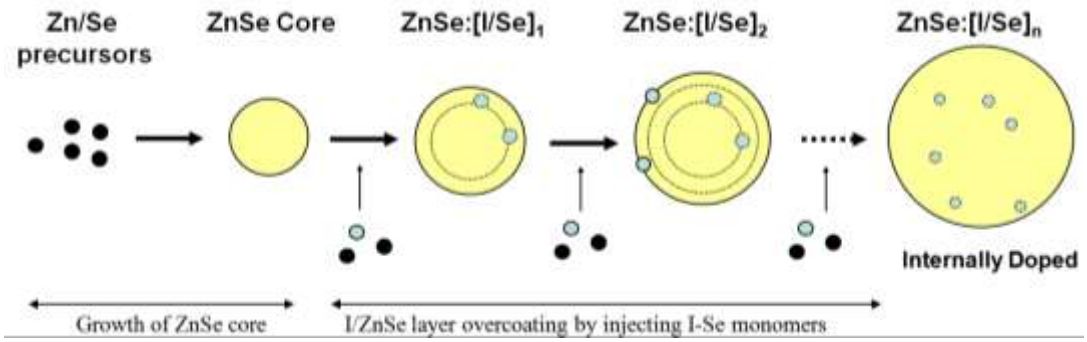

Figure S 1 Incorporation of impurities in QD matrix by layer-by-layer (LBL) doping.

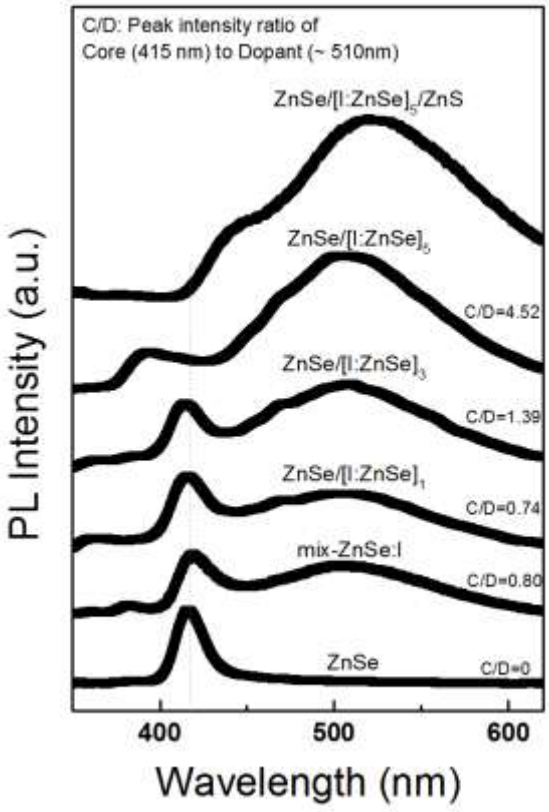

(a)

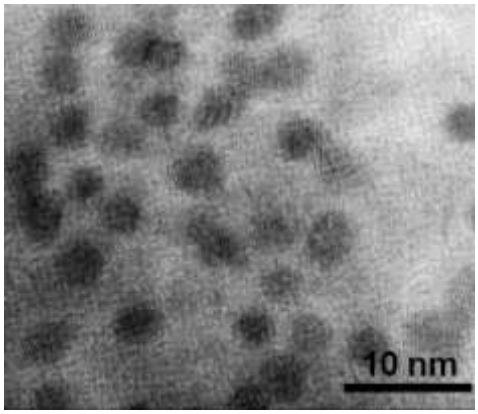

(b)

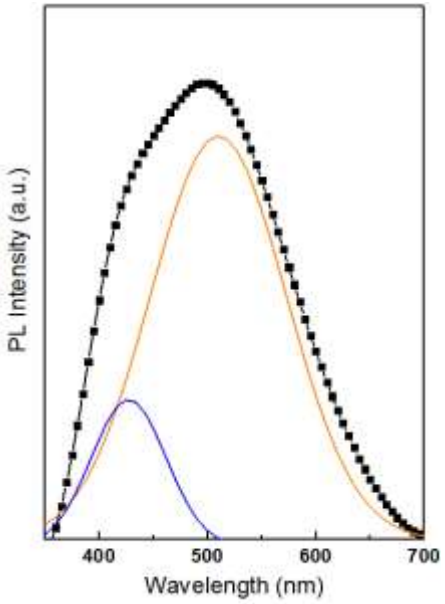

(c)

Figure S 2 ZnSe QDs synthesized by the hot injection method using ZnO as the Zn precursor.[1,2] (a) PL spectra from bare ZnSe QDs and I-doped ZnSe QDs by *insitu* overcoating. (b) TEM image of spherical ZnSe QDs. (c) PL spectra from intrinsic (undoped) non-spherical ZnSe QDs.

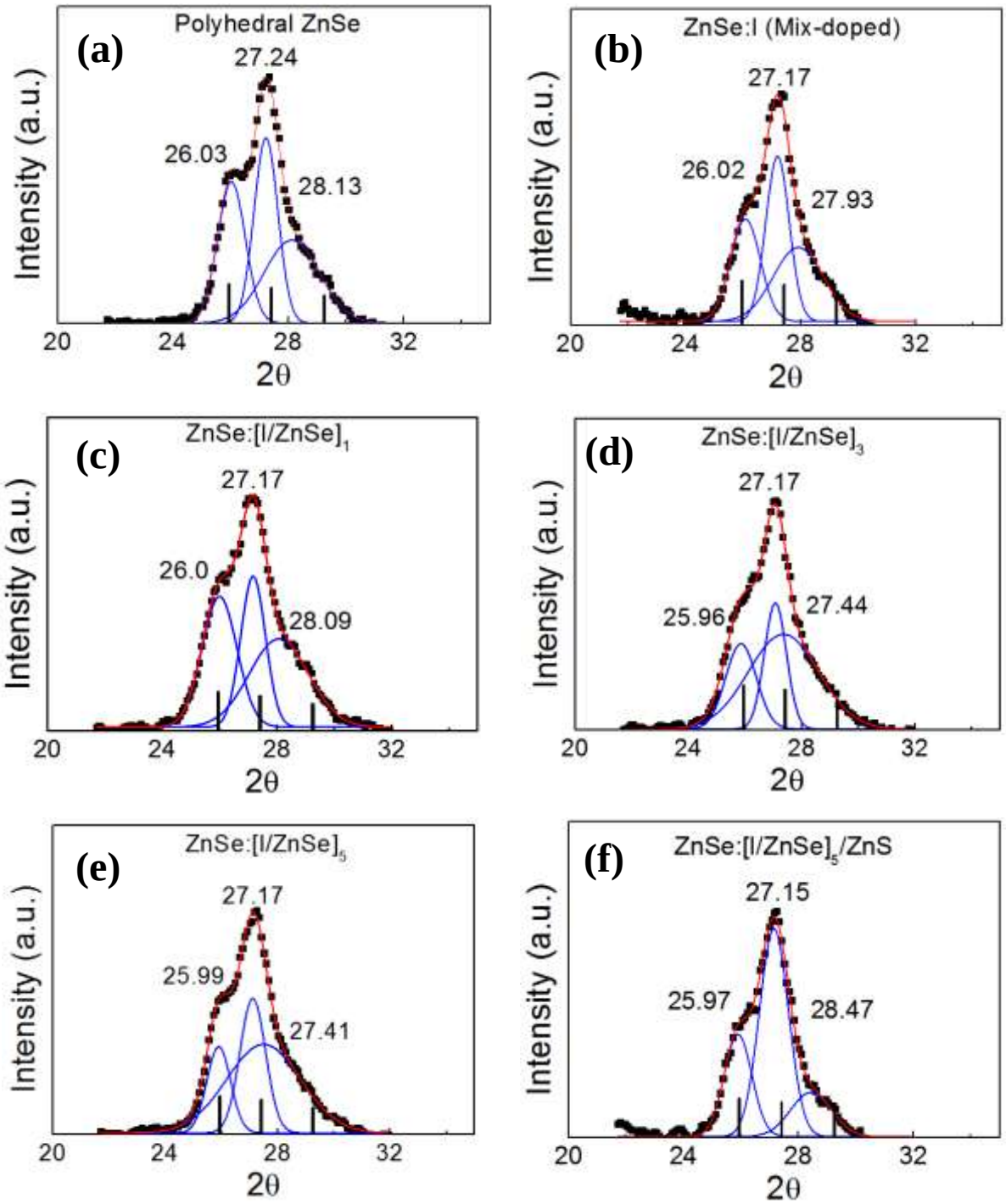

Figure S 3 XRD patterns of non-spherical (polyhedral) ZnSe QDs (a), ZnSe:I QDs from mix-doping (b), ZnSe:$[I/ZnSe]_1$ QDs (c), ZnSe:$[I/ZnSe]_3$ QDs (d), ZnSe:$[I/ZnSe]_5$ (e), and ZnSe:$[I/ZnSe]_5$/ZnS QDs (f) synthesized from Zn acetate. The blue curves are deconvolution of the patterns with Gaussian function.

Deconvolution of PL spectra. Deconvolution of PL spectra from intrinsic ZnSe, ZnSe:I, and ZnSe:$[I/ZnSe]_n$ QDs (Figure S1-S8) was performed by using 1 to 10 Gaussian functions to regenerate fit curves. For converged fittings, the curves with the minimum R-Square values (> 0.99 for all curves) are chosen. For curve in h, only three curves are successfully regenerated. The fitting results are summarized in the table shown below. The positions of the fitted peaks are related to possible mechanisms according to literature.

Table S1 Data extracted from fitting of PL spectra from ZnSe, ZnSe:I, and ZnSe:$[I/ZnSe]_n$ QDs. The "●" means peak relatively predominant compared with "◯". The numbers below the symbols are the peak position of the fit curves.

	Spherical				Polyhedral					
nm	Intrinsic	Mix doping	LBL doping		Intrinsic	Mix doping	LBL doping		Possible mechanisms according to literature	
			n=3	n=5			n=3	n=5		
< 400		◯ 360/382	◯ 360/380			◯ 383			Monomers, small particles	Excitonic Emission
~ 415	● 415	● 416	● 415		● 417	◯ 415	◯ 416		Core (QCE) (ref. 2)	
420-450		● 421/428	◯ 430	◯ 435						
450-500		● 466/499	● 472/490	● 453	● 458/488	● 459/490	◯ 463		DAP centers (ref. 3)	
500-530		● 530	● 505	● 485	● 518	● 510	◯ 530		Lattice defects (ref. 4)	Deep Level Emission
530-570		◯ 557	● 530	● 519/559	● 564	● 550	● 558	● 544		
570-620		◯ 590	◯ 572	● 592	◯ 602	◯ 590/638	● 595	● 585	Iodine/Impurity SA (ref. 5)	
620-700					◯ 632	◯ 638	● 652	● 642	Deep level centers	
> 700					◯ 786	◯ 767			Deep level centers	

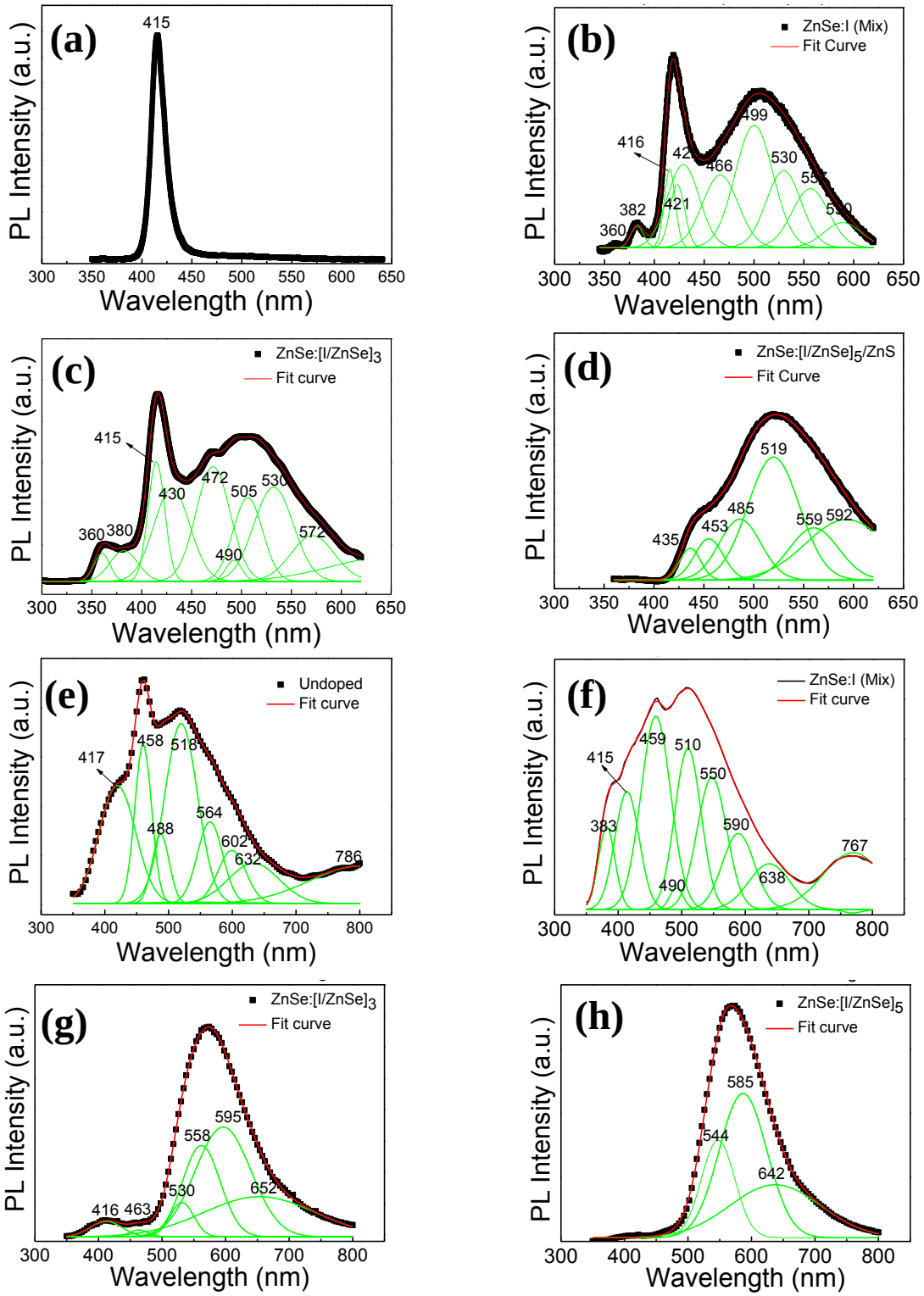

Figure S 4 PL spectra from spherical ZnSe QDs (a-d) prepared from ZnO and polyhedral ZnSe:$[I/ZnSe]_n$ QDs prepared from Zn acetate (e-h). The curves are fitted by Gaussian function and the red curve is a regenerated curve. (a) Spherical undoped ZnSe QDs. (b) Spherical ZnSe:I QDs prepared by the monomers-mixing method. (c) Spherical ZnSe:$[I/ZnSe]_3$ QDs doped by the LBL-doping method. (d) Spherical ZnSe:$[I/ZnSe]_5$/ZnS QDs prepared by the LBL-doping method. (e) Non-spherical undoped ZnSe QDs. (f) Non-spherical ZnSe:I QDs prepared by monomers-mixing-doping method. (g) Non-spherical ZnSe:$[I/ZnSe]_3$ QDs prepared by the LBL-doping method. (h) Non-spherical ZnSe:$[I/ZnSe]_5$ QDs prepared by the LBL-doping method. Only three curves are accepted to regenerate the experimental data.

Etching of ZnSe:(I/ZnSe)$_n$ QDs by pyridine. To investigate the doping, etching experiment is carried out for examining PL from the iodine-doped ZnSe QDs. As pyridine could remove a certain degree of surface species via the ligand exchange process, it provides a convenient way to observe the surface or internal doping. The etching for spherical ZnSe:(I/ZnSe)$_1$ QDs does not significantly vary the deep-level peak (506 to 502 nm), while there is a blue shift from 518 to 505 nm for ZnSe:(I/ZnSe)$_{10}$, which shows that the doping layers made more contribution to the lower energy emission band. Both of the etched spherical samples have similar PL profiles to that of surface-doped samples. The result of polyhedral ZnSe:(I/ZnSe)$_5$ etched by pyridine is similar. The intensity of the iodine-related PL peak significantly reduces and the peak position also shifts to lower wavelength region but higher wavelength emission still remains.

Experimental. Dried samples were dispersed into 50 ml pyridine in an ultrasonic bath at 50 ^{o}C for 3 hours. The samples were collected by adding 1 ml of hexane before centrifugation and dried by vacuum. Photoluminescence (PL) measurement was performed at 325-nm excitation wavelength.

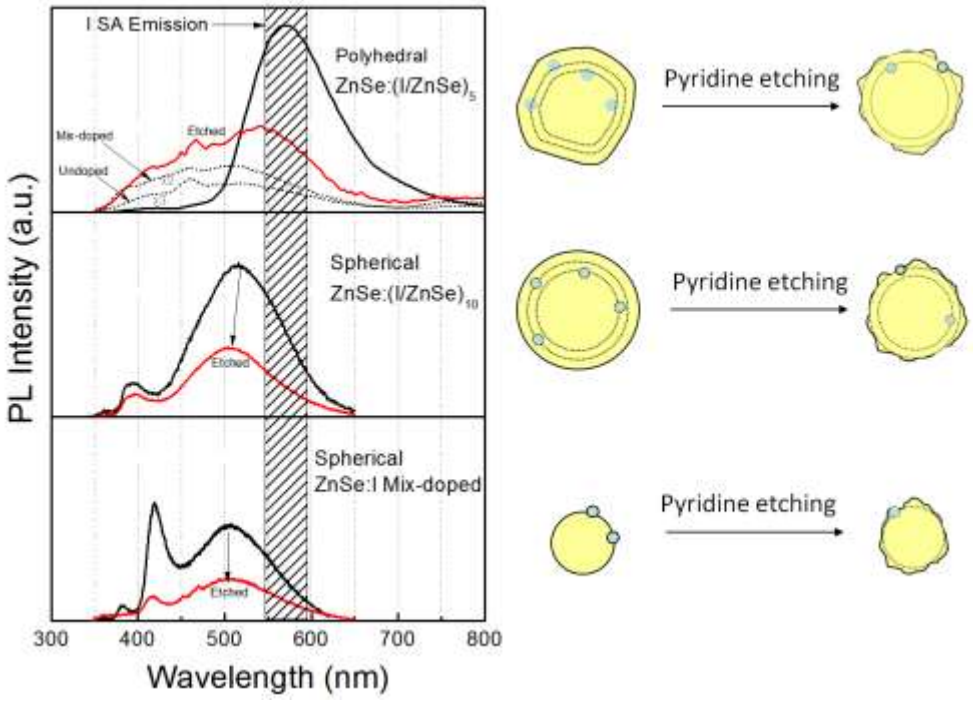

Figure S 5 PL spectra of spherical and polyhedral ZnSe QDs doped by iodine etched by pyridine. The right illustration shows etching of the QDs surface.

Table S2 ICP-AES (Jarrell-Ash, ICAP 9000) of spherical and polyhedral ZnSe and doped ZnSe QDs

samples/at%	Spherical				Polyhedral			
	Zn	Se	I	S	Zn	Se	I	S
ZnSe	0.502	0.498	0	0	0.505	0.495	0	0
ZnSe-mix	0.496	0.495	0.009	0	0.498	0.49	0.012	0
ZnSe-mix-etched	0.521	0.477	0.002	0	0.522	0.478	0	0
ZnSe:$[I/ZnSe]_5$	0.481	0.464	0.055	0	0.481	0.448	0.071	0
ZnSe:$[I/ZnSe]_5$-etched	0.503	0.482	0.015	0	0.498	0.481	0.021	0
Core/shell ZnSe/ZnS	0.478	0.465	0	0.057	-	-	-	-

PL decay. PL decay of ZnSe QDs shows that five doping layers results in a much faster PL decay for ZnSe:$(I/ZnSe)_5$ QDs than either mixed-doped or intrinsic ZnSe QDs, indicating more impurity atoms introduced to ZnSe:$(I/ZnSe)_5$ QDs compared with intrinsic ZnSe and surface-doped ZnSe:I QDs.

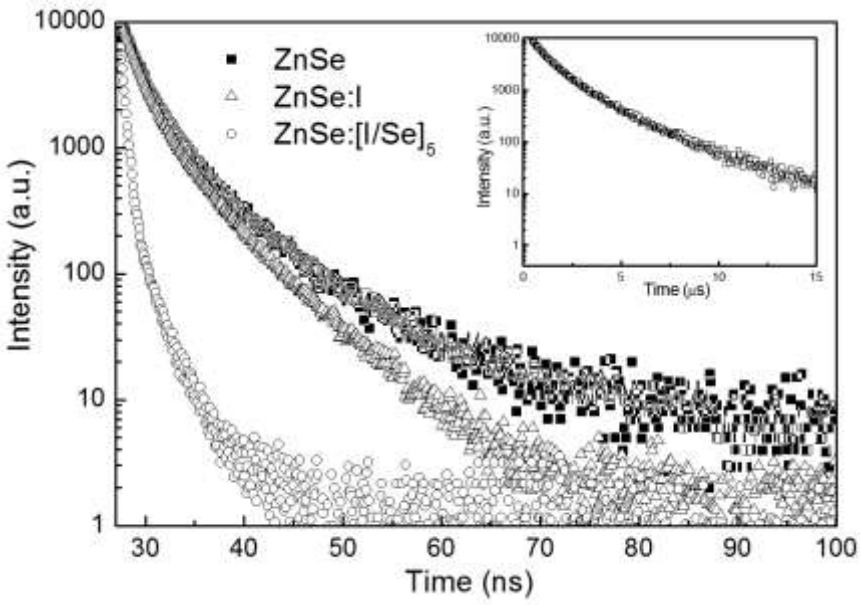

Figure S 6 PL decay curves of ZnSe, ZnSe:I, and ZnSe:$[I/ZnSe]_5$ QDs monitored at 400-430 nm. The inset shows PL decay monitored at 500-700 nm for ZnSe:$[I/ZnSe]_5$ QDs. Samples were excited at 375 nm (IBH NanoLED-375L).

References

[1] (a) Chen, H. S.; Lo, B.; Hwang, J. Y.; Chang, G. Y.; Chen, C. M.; Tasi, S. J.; Wang, S. J. J. *J. Phys. Chem. B* **2004**, *108*, 17119. (b) Chen, H. S.; Horng, H. Y.; Kumar, R. V. *Appl. Phys. Lett.* **2009**, *94*, 141107.

[2] (a) Chen, H. S.; Wang, S. J. J.; Lo C. J.; Chi, J. Y. *Appl. Phys. Lett.* **2005**, *86*, 131905. (b) Lutich, A. A.; Mauser, C.; Como, E. D.; Huang, J.; Vaneski, A.; Talapin, D. V.; Rogach, A. L.; Feldmann, J. *Nano Lett.* **2010**, *10*, 4646. (c) Choi, C. L.; Li, H.; Olson, A. C. K.; Jain, P. K.; Sivasankar, S.; Alivisatos, A. P. *Nano. Lett.* **2011**, *11*, 2358.

[3] Thomas, A. E.; Russell, G. J.; Woods, J. *J. Phys. C: Solid State Phys.* **1984**, *17*, 6219.

[4] Massa, J. S.; Buller, G. S.; Walker, A. C.; Simpson, J.; Prior, K. A.; Cavenett, B. C. *Appl. Phys. Lett.* **1995**, *67*, 61. (b) Mullins, J. T.; Horsburgh, G.; Simpson, J; Thompson, P.; Taghizadeh, M. R.; Hauksson, I.; Wang, S. Y.; Prior, K. A.; Cavenett, B.C.; Williams, G. M.; Cullis, A. G. *J. Cryst. Growth* **1994**, *138*, 357-361. (c) Massa, J. S.; Buller, G. S.; Walker, A. C.; Simpson, J.; Prior, K. A.; Cavenett, B. C. *Appl. Phys. Lett.* **1994**, *64*, 589-591. (d) Massa, J. S.; Buller, G. S.; Walker, A. C.; Simpson, J.; Horsburgh, G., Mullins, J. T.; Prior, K. A.; Cavenett, B. C. *J. Cryst. Growth* **1996**, *159*, 402-405. (e) Wallace, J. M.; Simpson, J.; Wang, S. Y.; Stewart, H.; Hunter, J. J.; Adams, S. J. A.; Prior, K. A.; Cavenett, B. C. *J. Cryst. Growth* **1992**, *117*, 320-323. (f) Simpson, J.; Wallace, J. M.; Wang, S. Y.; Stewart, H.; Hunter, J. J.; Adam, S. J. A.; Prior, K. A.; Cavenett, B. C. *Semicond. Sci. Technol.* **1992**, *7*, 464-466.

[5] (a) Fujiwara, S.; Namikawa, Y.; Nakamura, T.; Tatsumi, M. *J. Cryst. Growth* **2005**, *275*, e415. (b) Muranoi, T.; Onizawa, S.; Sasaki, M. *J. Cryst. Growth* **1994**, *138*, 255. (c) Shibata, N.; Ohki, A.; Katsui, A. *J. Cryst. Growth* **1988**, *93*, 703. (d) Shibata, N.; Ohki, A.; Zembutsu, S. *Jpn. J. Appl. Phys.* **1988**, *27*, L251.